Microelectronic Engineering 158 (2016) 85–90

Contents lists available at ScienceDirect

Microelectronic Engineering

journal homepage: www.elsevier.com/locate/mee

# Three-dimensional imaging approach using built-in lens mask lithography

Toshiki Tanaka, Hisao Kikuta, Hiroaki Kawata, Masaaki Yasuda, Masaru Sasago, Yoshihiko Hirai *

*Osaka Prefecture University, Graduate School of Engineering, Department of Physics and Electronics Engineering, Sakai, Osaka 599-8531, Japan*

ARTICLE INFO

*Article history:*
Received 8 November 2015
Received in revised form 22 February 2016
Accepted 8 March 2016
Available online 16 March 2016

*Keywords:*
Photolithography
Complex amplitude
Mask
Phase
Multi-focus

ABSTRACT

Three-dimensional imaging using a complex transparency mask called a built-in lens mask is proposed in this paper. The mask is designed to have multiple focal planes at arbitrary depths for the seed patterns that form partial components of the three-dimensional structure. Three-dimensional imaging is demonstrated by the superposition of these seed patterns at various depths. Using computational lithography, the optical intensity profiles in space are demonstrated for several characters, and their three-dimensional imaging is confirmed. The separation characteristics of the optical images in the depth direction and the discretization of the complex transmittance of the built-in lens mask is discussed.

© 2016 Elsevier B.V. All rights reserved.

## 1. Introduction

Three-dimensional (3D) microfabrication processes are in increasing demand for fabrication of advanced microfluidic devices and micro-optical components. Also, 3D microstructures are proving valuable for functional structures such as complex biomimetic structures and permanent 3D holographic memory structures. Several approaches have been proposed for 3D micro- and nanostructure fabrication. Si-based semiconductor fabrication methods based on layer-by-layer fabrication methods using sacrificial layers represent the typical classical approach [1]. In contrast, novel 3D micro- and nanofabrication processes using beam-based processing have been proposed. Focused ion beam deposition techniques [2] and multi-beam exposure using two-photon absorption [3] have been used to realize nanoscale fine structures. Also, 3D structures formed by nanoimprint techniques [4,5] or by a multiple exposure technique [6] based on conventional photolithography have been demonstrated for mainly periodic structures. Recently, microdevice fabrication has also been demonstrated using 3D printer systems [7]. However, these conventional methods encounter difficulties when applied to the mass production of advanced devices, and a simple and effective lithographic method is required for 3D microscale processes.

In addition, novel 3D photolithography approaches based on single shot exposure through a photomask and using proximity correction have been developed, including inverse lithography [8], holographic lithography [9–11], and diffraction-based exposure [12].

In our previous work, we proposed deep focus imaging using conventional proximity exposure systems by built-in lens mask lithography [13] with a complex transmittance mask, as derived below.

When the required (i.e., designed) optical image at the image plane $u_0(x,y,d)$ is provided, the complex optical amplitude of the plane wave $\overline{A}_0$ propagating in the $k=(k_x,k_y)$ plane is expressed as

$$\overline{A}_0(k_x,k_y)=\begin{cases}\iint u_0(x,y,d)\exp[i(k_xx+k_yy)]dxdy : for\ \sqrt{k_x^2+k_y^2}\le\dfrac{2\pi}{\lambda}\sin\theta\\ 0 : for\ \sqrt{k_x^2+k_y^2}>\dfrac{2\pi}{\lambda}\sin\theta\end{cases} \tag{1}$$

where $d$, $\lambda$, and $\theta$ are the distance from the mask plane (X,Y), the optical wavelength in free space, and the angular aperture, respectively.

An equivalent wave propagation plane in the z plane is then expressed as

$$A_0(k_x,k_y,z)=\overline{A}_0(k_x,k_y,z)\exp\left[i\sqrt{k^2-\left(k_x^2+k_y^2\right)}z\right]. \tag{2}$$

The optical complex amplitude $g_0$(X,Y), i.e., the amplitude and the phase shift at the (X,Y) plane, is then obtained as

$$g_0(X,Y)=1/(2\pi)^2\iint_{\sqrt{k_x^2+k_y^2}\le\frac{2\pi}{\lambda}}A_0(k_x,k_y,d)\exp[-i(k_xx+k_yy)]dk_xdk_y. \tag{3}$$

When we place an optically transmissive plate with amplitude and phase $g_0$(X,Y) under coherent light irradiation, the wave optical

* Corresponding author at: Osaka Prefecture University, Graduate School of Engineering, Department of Physics and Electronics Engineering, Sakai 599-8531, Japan. Tel.: +81 072 254 9267; fax: +81 072 254 9908.
*E-mail address:* hirai@pe.osakafu-u.ac.jp (Y. Hirai).

http://dx.doi.org/10.1016/j.mee.2016.03.022
0167-9317/© 2016 Elsevier B.V. All rights reserved.

propagation plane can be emulated. As a result, the arbitrary optical intensity profile $u_0(x,y,d)$ at the image plane can be obtained via the optical transmittance plate with the amplitude and phase shift of the complex function $g_0(X,Y)$ using the built-in lens mask.

The principle of built-in lens mask lithography has been confirmed by both computational lithography [14,15] and experimental studies.

In this paper, we propose a 3D imaging method using a single mask without the multiple exposures used by conventional proximity exposure systems. Computational lithography is used to verify the performance of and the issues related to this 3D imaging approach.

## 2. 3D imaging using built-in lens mask

Use of the built-in lens mask means that the focus plane can be arbitrarily designed as shown in Fig. 1(a), because it allows us to design the depth of focus and the image profile. The built-in lens mask was explained in detail in our previous work [13]. Using the flexibility of the built-in lens mask, a 3D imaging method using a single mask exposure is proposed here. The method is based on the superposition of masks with various focal planes for a multiple focusing approach. Fig. 1(b) schematically illustrates the multiple focusing method by showing the superposition of the complex transmittances of each mask to produce arbitrary focus planes.

In the 3D imaging approach, the original 3D structure is divided into seed patterns $u_n$ at arbitrary depths. The complex transmittance $g_n$ for each seed pattern $u_n$ is designed in the conventional manner. The complex transmittances are then superposed, as expressed using Eq. (4), into a single mask.

$$g_0^* = \sum_i g_i^* e^{\Delta\theta}/N \tag{4}$$

Here, $N$ is the number of seed patterns. In this case, the phase of the built-in lens mask for each seed pattern is shifted by $\Delta\theta$ to prevent interference between the seed patterns.

## 3. Computational lithography results and discussions

Spatial imaging using the proposed method has been studied using a computational lithography approach [13–15]. The exposure wavelength used is 365 nm. The optical transmittance and the phase of the complex transmittance $g_0^*$ are alternated continuously. First, we discuss 3D imaging using a continuum complex index mask as an ideal case. Then, we discuss the realization of a discretized complex index mask for feasible mask systems using conventional phase shift mask technology. We first discuss imaging in an air-filled space, i.e., the refractive index $n_{space}$ in the space is 1.0, as for air. Then, we consider the prospects for proximity exposure of the resist.

### 3.1. Spatial imaging using continuum complex index mask in air-filled space

Using the proposed method, imaging of the letter A is demonstrated, as shown in Fig. 2. The focal depths of the seed patterns have five levels and the pattern width in the lateral direction is 1.0 μm, as shown in Fig. 2(a). The spacing of the seed pattern layer in the depth direction is 12.5 μm. Fig. 2(b) shows the spatial optical image, where the complex transmittances of the individual seed patterns are simply superposed. The lower lateral bar of the letter A is missing. This could be caused by interference with the seed pattern of the top bar. To recover the missing bar, the related transmittance phase at the lower lateral bar in the letter A is shifted by π radians, as shown in Fig. 3(a). The missing lateral bars are then successfully recovered, as shown in Fig. 3(b).

Next, we briefly investigate the separation performance using the representative case shown in Fig. 4. In this case, the spatial separation between two parallel lines is investigated from the perspective of a design rule. The upper line is placed at a depth of 20 μm and the spacing

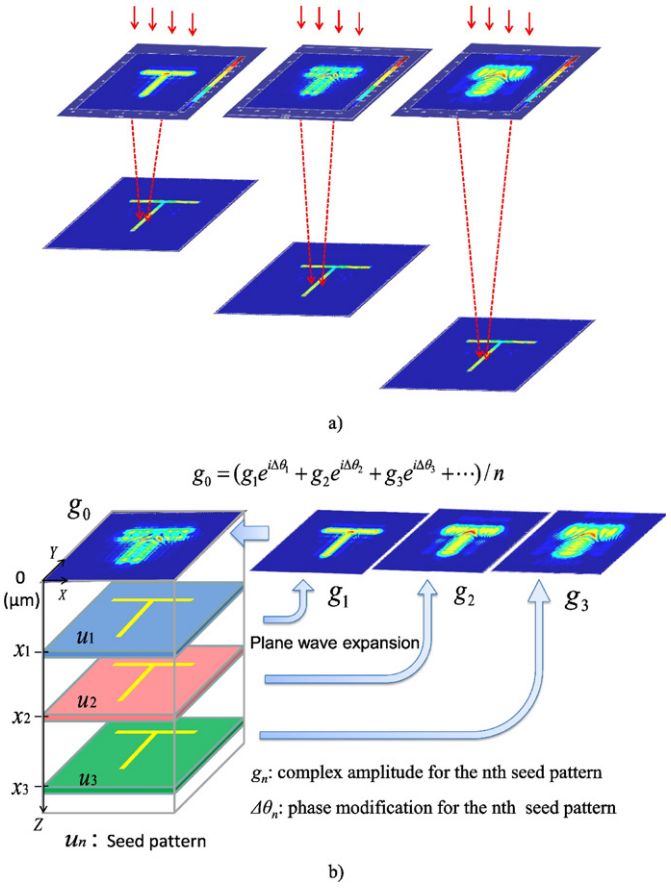


**Fig. 1.** Schematics of three-dimensional focusing processes using built-in lens masks. a) Single focusing by individual built-in lens mask on arbitrary focus plane. b) Multiple focusing mask produced by superposition of several built-in lens masks for arbitrary seed patterns.

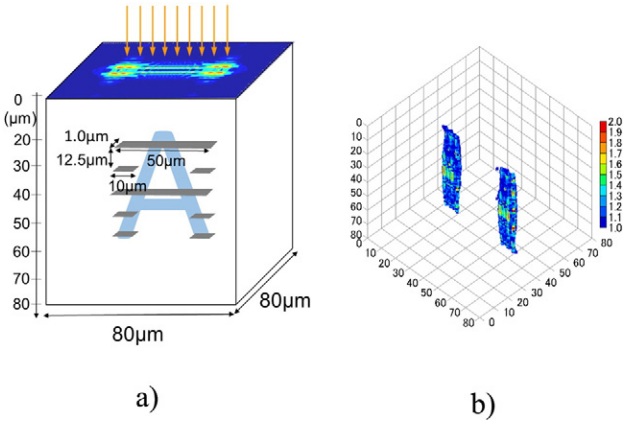


**Fig. 2.** Three-dimensional imaging of letter "A" without phase modification. a) Layout of seed patterns. b) Spatial optical intensity profile.

Download English Version:

https://daneshyari.com/en/article/541155

Download Persian Version:

https://daneshyari.com/article/541155

Daneshyari.com